Technical Report No. 32-652

JPL Intense Field Air Core Magnet

Rudolph Rust

D. D. Elleman

R. M. Noble

jpl

JET PROPULSION LABORATORY

CALIFORNIA INSTITUTE OF TECHNOLOGY

PASADENA, CALIFORNIA

August 31, 1964

Technical Report No. 32-652

JPL Intense Field Air Core Magnet

Rudolph Rust

D. D. Elleman

R. M. Noble

R. E. Covey

R. E. Covey, Chief
Space Simulators and Facility Engineering Section

JET PROPULSION LABORATORY
CALIFORNIA INSTITUTE OF TECHNOLOGY
PASADENA, CALIFORNIA

August 31, 1964

Prepared Under Contract No. NAS 7-100
National Aeronautics & Space Administration

CONTENTS

TABLES

FIGURES

FIGURES (Cont'd)

ABSTRACT

An intense magnetic field facility has been completed at the Jet Propulsion Laboratory (JPL). This project was initiated by the Physics Section of the Space Sciences Division. Engineering responsibility for the magnet design, fabrication, and subsequent laboratory completion was vested in the Project Engineering Group of the Space Simulators and Facility Engineering Section. This Report gives descriptive information summarizing major system design considerations and an evaluation of the recently completed magnet facility.

Author

I. INTENSE MAGNETIC FIELD LABORATORY

The first and most important item in a magnet laboratory is a stable power supply. Magnets producing field strengths of 100,000 gauss must not contain ferrous materials. In order to produce continuous fields near 100 kilogauss in a 2.5-in. bore magnet, approximately 2 Mw of dc power must be used. As shown in Fig. 1, considerations of the design of this magnet indicate that input power must be heavy current at low voltage. The copper solenoid purity is 95% IACS, consequently magnet resistance is of the order of 220 $\mu\Omega$ at an operating temperature of 60°C (140°F). This minimizes the temperature requirements on the electrical insulation spacers placed between the coil turns.

For this installation, a new unipolar motor generator set developing 2.4 Mw dc is used. The test room containing the magnet is visible for communication from the control panel of the motor generator set since it is not in the same room. The magnet was placed as near to the generator as possible in order to minimize the amount of copper required for electrical busses to carry approximately 95,000 amp at 21 v during operation.

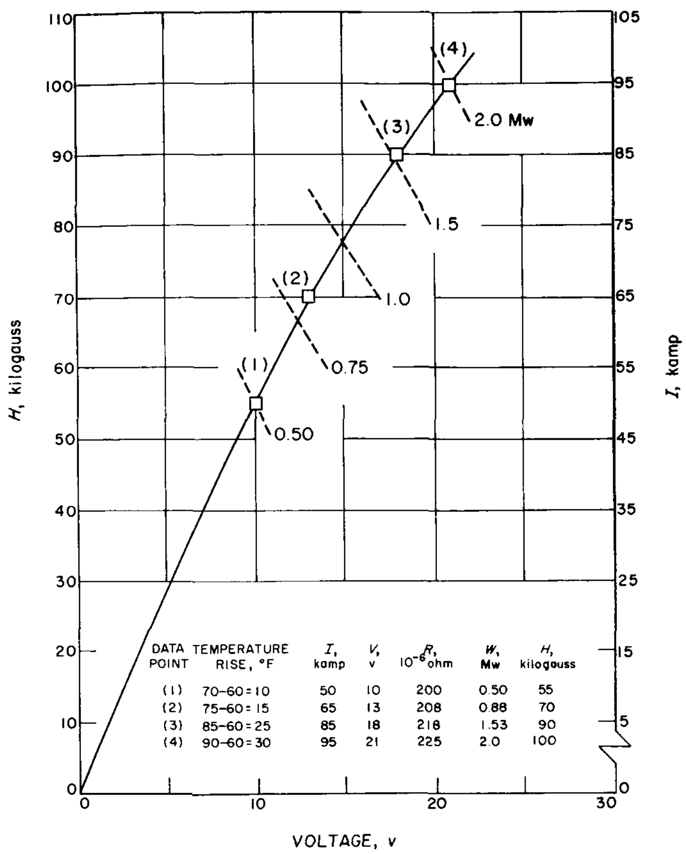

DATA POINT	TEMPERATURE RISE, °F	I, kamp	V, v	R, 10^{-6} ohm	W, Mw	H, kilogauss
(1)	70–60 = 10	50	10	200	0.50	55
(2)	75–60 = 15	65	13	208	0.88	70
(3)	85–60 = 25	85	18	218	1.53	90
(4)	90–60 = 30	95	21	225	2.0	100

Fig. 1. Magnet performance data

II. THE POWER SUPPLY

The central item in the power supply is the unipolar motor generator set shown in Fig. 2. The dc generator nominally puts out 2.4 Mw. It has a novel liquid metal (NaK) current collection system replacing conventional dc generator brushes. A 2500-hp induction motor developes about 3500 hp continuously by operating with 140% load factor on the three phase current at 4160 v. The motor turns at 1785 rpm and is physically attached to the unipolar generator via a 1:4 speed increase gear box attached to a common bedplate. Electrical controls are interlocked with such necessary items as water flow to the magnet and magnet-bus, NaK flow and temperature in the generator, lube-oil flow and temperature to bearings, etc. The unipolar generator output voltage can be raised or lowered by holding down on a control button at the control panel (Fig. 3). The generator's internal resistance is approximately 5 $\mu\Omega$. This provides a constant voltage or zero-impedance characteristic whereby the system current is determined only by the load (magnet) resistance.

Very low-impedance systems offer more benefits for high-powered electromagnets than high-impedance systems. The greatest concern is the voltage-to-current ratio

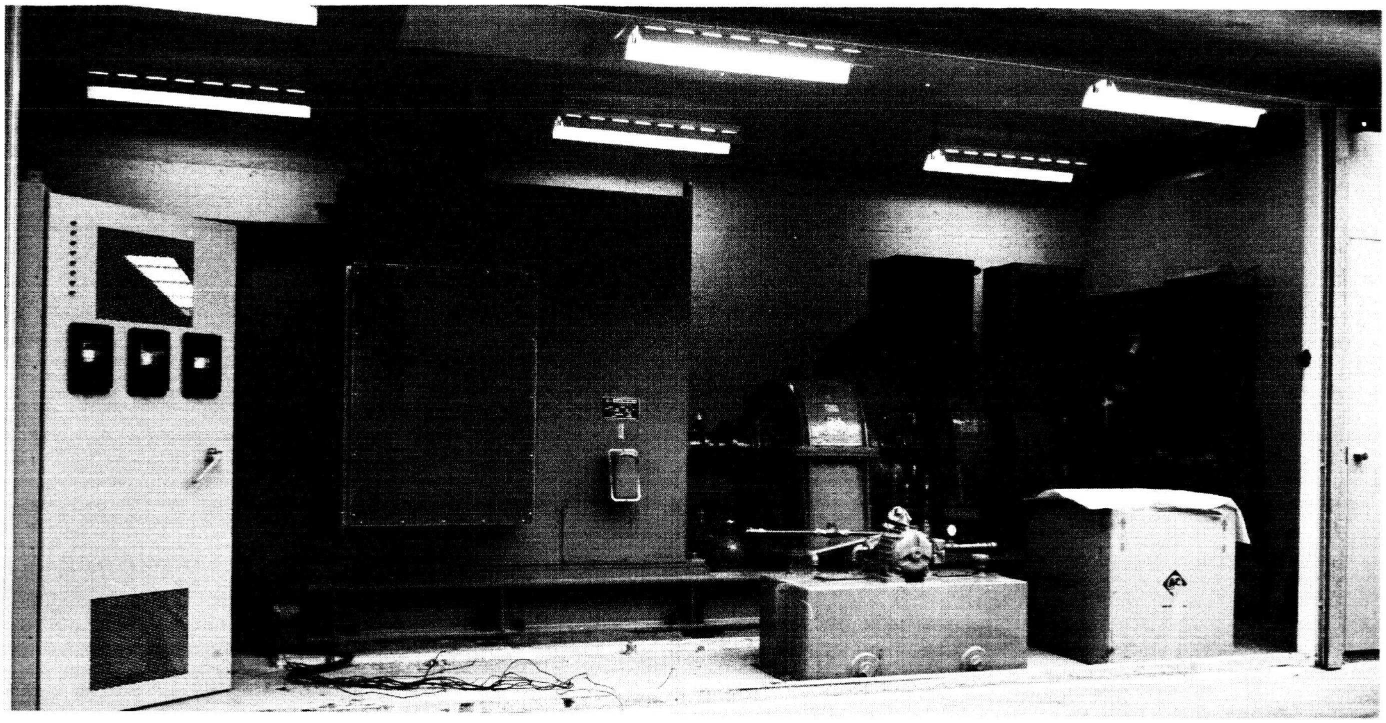

Fig. 2. Motor generator set power supply

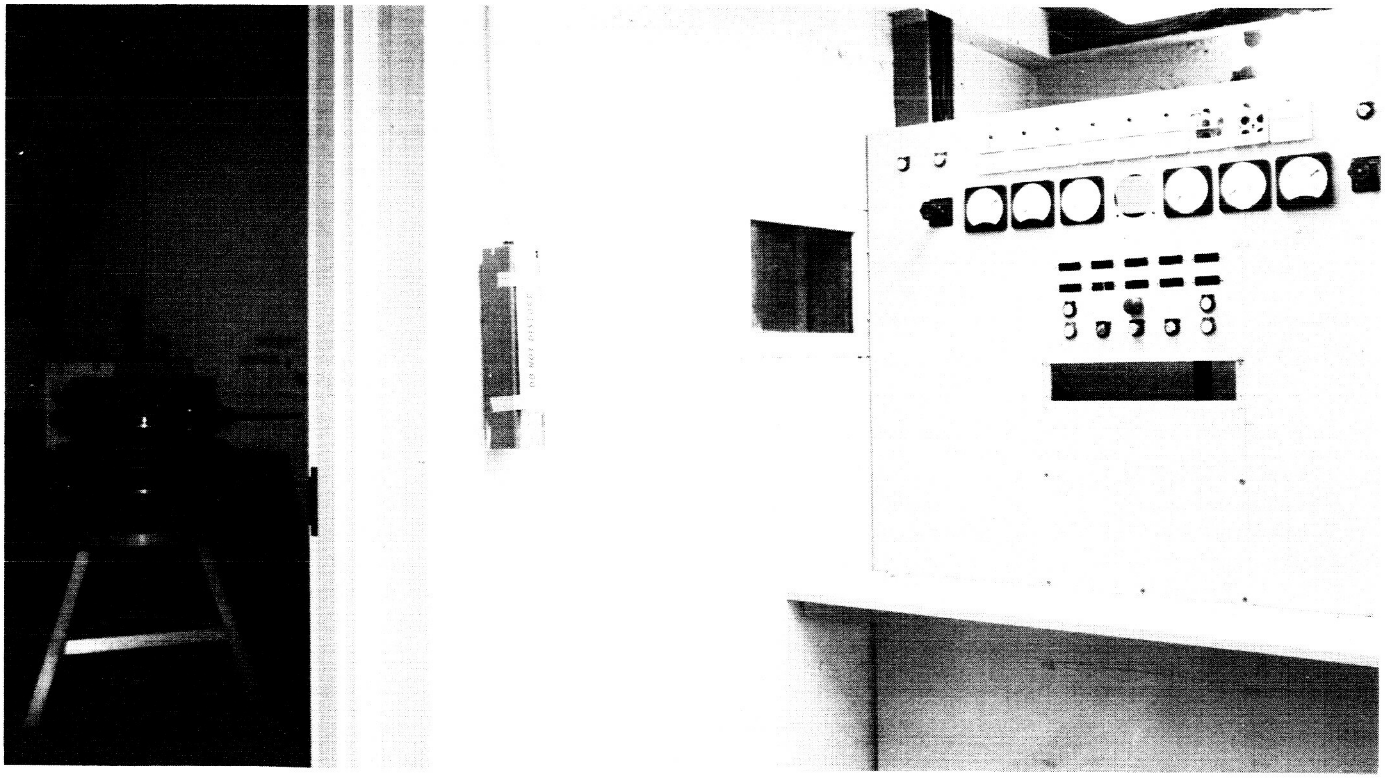

Fig. 3. Control panel

of the power supply and its consequent influence on magnet design. Several arguments in favor of the above allegations are:

1. The inherent bulk strength of thicker coil turns aid in withstanding ponderomotive forces (i.e., electrically produced mechanical stresses) within the solenoid.
2. Distilled water containing sodium nitrite can be used from existing wind tunnel facilities. The JPL low-impedance magnet has a turn-to-turn potential difference of 0.8 v. Thus, even with very low-grade insulating materials, the magnet operates on what is probably the most electrically conductive water presently used in any high-field laboratory.
3. Large cryogenically cooled magnets can be contemplated in the future. The very low conductor resistance of such devices will require a high-current, low-impedance, power source.

Arguments against the use of low-impedance power supplies are:

1. The electrical bus that couples the magnet to the motor generator set is large in conductor area.
2. The high inductance of unipolar machines prevent their use for rapid pulse rise magnets such as those powered by capacitance discharge.

Two methods exist for producing 2.0 Mw of dc power at low voltage. One method consists of using transformers for reducing the line voltage along with rectifiers and filters. The other method is to use a Faraday type homopolar generator. This is the basic design of the JPL "unipolar" generator. A unipolar generator differs from a conventional dc machine in several ways. A conventional machine has carbon brushes. Commutating bars form the armature windings, and relatively high friction exists. Conversely, a unipolar machine, as the name implies, has only one armature conductor and no commutator, no magnetic core loss, and relatively low windage and friction. This results in approximately 98% efficiency as compared to around 88% for conventional dc machines. Also, excitation requirements are very low—around 0.1% of the machine's kw output.

The NaK alloy used in the machine has a proportion of approximately 44% potassium and 56% sodium, with a freezing point of 7°C and a boiling point of 784°C. Approximately 60 lb of NaK are used in the two current collection rings. Each collector system consists of a storage sump, a circulating pump, and an NaK-to-air heat exchanger. The generator and NaK systems have a maintained nitrogen atmosphere. Extreme care is required in handling the NaK since it reacts violently with water, carbon tetrachloride, carbon dioxide, and many other compounds. All necessary safety and fire prevention equipment is available near the motor generator set.

III. THE ELECTRIC BUS

The facility layout was designed to minimize the length of the bus required between the generator and magnet. Easy access to all equipment resulted in about a 6-ft length.

Design criteria for the bus included: (a) low voltage drop of 1 v at 100,000 amp, (b) resistance stability, (c) strength enough to withstand forces due to high currents, and (d) small enough to attach the generator and magnet busplates.

The final system is shown in Fig. 4. Each polarity consists of six water-cooled cables, each with six conductors approximately 700 mcm inside a 4¼-in. hose. The cooling water enters from one end, and exits on the other, at a flow rate of approximately 15 gal/min. Each conductor resistance is approximately 15 $\mu\Omega$, resulting in a 2.8-$\mu\Omega$ resistance for the six parallel conductors. The bus then represents about a 3% loss with the magnet resistance.

Each conductor has a connector with 17.5 square inches of contact surface, and at 100,000-amp current, this results in 1,000 amp/in.^{2} contact current density. The surfaces were silver-plated and attached with high-strength corrosion-resistant silicon bronze bolts.

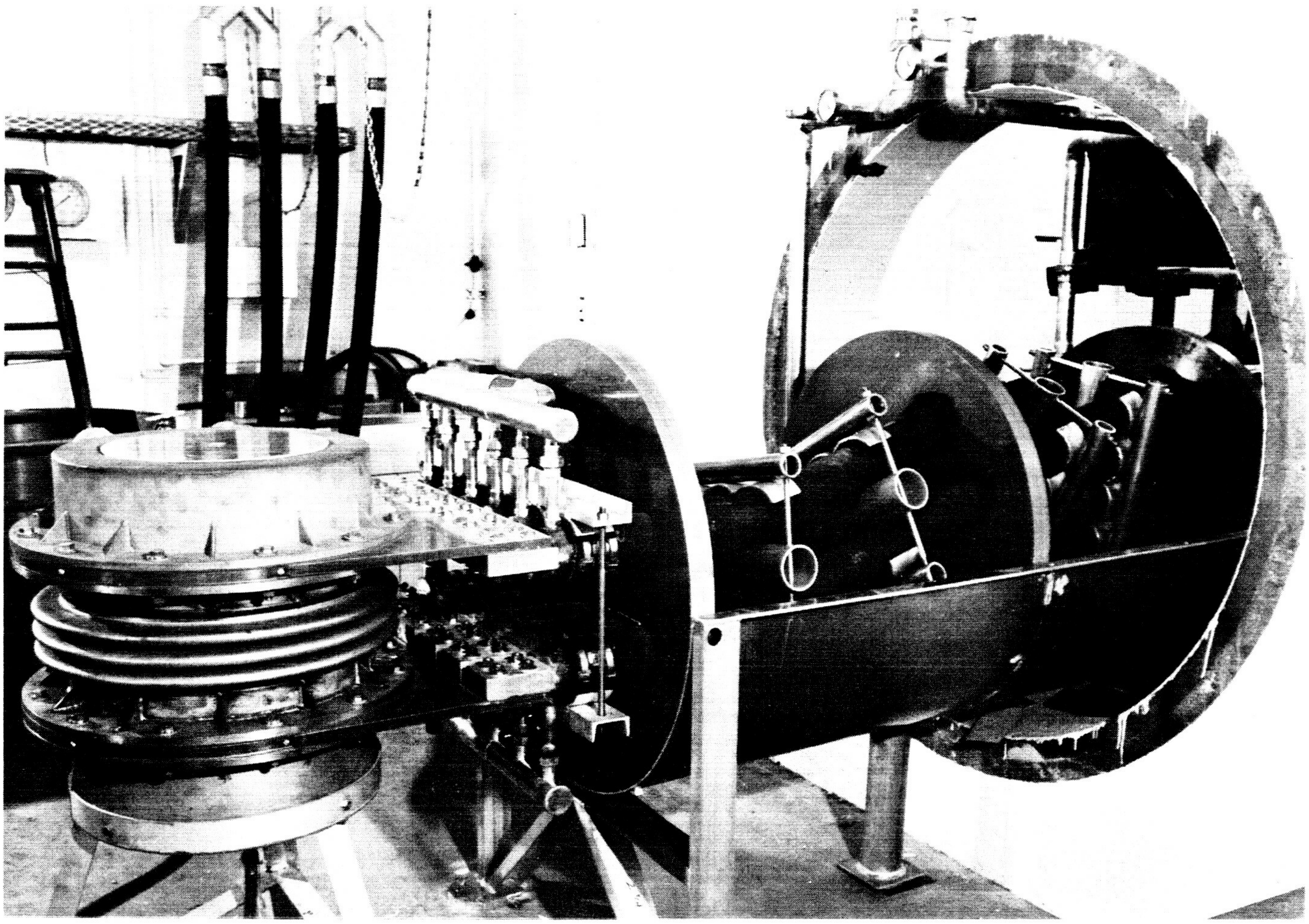

Fig. 4. Magnet and electric bus

Supports for the bus are also shown in Fig. 4. A 3-ft D aluminum cylinder with three 2-in. thick Micarta discs form the main supports. Four aluminum pipe supports are placed between the Micarta discs. These are to withstand the force tending to separate the busses due to the ponderomotive forces from high currents. This force was calculated to be 750 lb/lineal foot at 100,000 amp. It should be noted that the bus rotates 90 deg from the generator to the magnet. When current is flowing, the magnetic forces tend to "unwind" the bus due to the electrical torque. However, the 3-ft D cylinder and Micarta discs bolted together form an adequate constraint.

IV. THE WATER SUPPLY

Distilled water is pumped through the magnet, (Fig. 5) at a rate of about 440 gal/min. The capacity of the cooling circuit is great enough to keep the maximum distilled water temperature between 60°C (140°F) and 82°C (180°F), depending on initial water temperature. This is sufficient to keep the maximum temperature of the copper in the central bore section of the magnet to within a few degrees of the boiling point of water.

Heat transfer from a solid surface to a turbulent nonboiling liquid can be described by the relation (Ref. 1):

$$\mathrm{Nu} = 0.023\,\mathrm{Pr}^{0.4}\,\mathrm{Re}^{0.8} \qquad (1)$$

where, the dimensionless numbers Nusselt, Prandtl, and Reynolds appear in that order. Temperature differences between the liquid and metal obey the relation:

$$W = hA_c\,(\Delta T) \qquad (2)$$

where, W is the power dissipated from the solid, h is the interface heat transfer coefficient, and A_c is the total

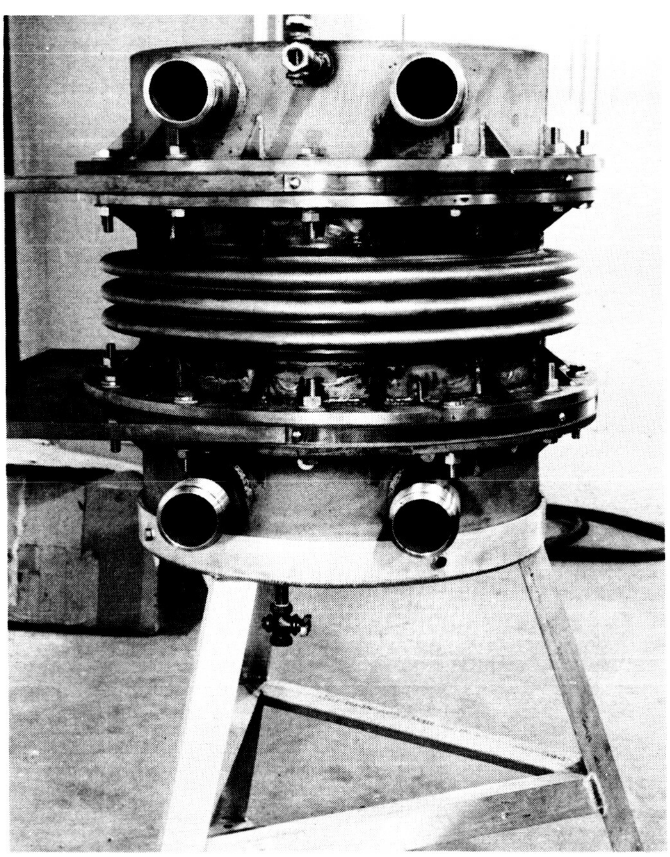

Fig. 5. Water holes in magnet assembly

cooling surface contact area between solid and liquid. Equations (1) and (2) can be combined to form the following expression:

$$\Delta T = (0.023)^{-1}\left(\frac{\mu}{Ck^{1.5}\,\rho^{2}}\right)^{0.4}\left[\frac{A_f^{0.8}\,d^{0.2}}{A_c}\right]\left[\frac{W}{V^{0.8}}\right] \qquad (3)$$

For temperatures near 25°C (77°F), the second term of this expression has the following factors: the viscosity (μ) = 0.00894 g/cm sec, the specific heat (C) = 4.18 j/g deg C, the density (ρ) = 0.997 g/cm^3, and the thermal conductivity of the cooling water (k) = 0.00606 w/cm deg C. Thus, the entire second term has a numerical value of 1.84 cm$^{2.6}$ sec $^{0.2}$ deg C/j. In the third term, the total frontal area of the cooling passages $A_f = 2\pi\, r_1\, h\, N$ $= 2\pi$ (1.25 in.) (0.025 in.) (27.6) (6.45 cm^2/in.^{2}) = 35 cm^2. The hydraulic diameter is defined as four times the frontal area of one channel divided by its wetted perimeter. After simplification, the hydraulic diameter, $d = 4$ $h = 4$ (0.025 in.) (2.54 cm/in.) = 0.25 cm. The total contact surface area between the solenoid and water, $A_c = \pi\,(r_2^2 - r_1^2)\,N = \pi$ (72 in.^{2} − 1.56 in.^{2}) (27.6) (6.45 cm^2/in.^{2}) = 39,400 cm^2. This area comprises about five times the surface area of a comparable "Bitter" solenoid. Thus, the entire third term has a numerical value of 3.31×10^{-4} cm$^{-0.2}$. The last term involves the total volume of liquid circulated per unit time. V = 430 gal/min = 27,100 cm^3/sec. The power requirement near 100 kilogauss is 2.0 Mw. Therefore, the last term has a numerical value of 568 w (sec$^{0.8}$) (cm$^{-2.4}$). Substituting this information into Eq. (3) gives the expected temperature rise of 15°C (27°F). During operation of the magnet near the 100 kilogauss level, the inlet and outlet water temperatures were monitored. As expected, the temperature rise was 87°F − 60°F = 27°F.

The water contains from 500 to 1500 ppm sodium nitrite for corrosion control. The low-voltage magnet system can tolerate such contaminants without very great electrical losses (see Table 1).

Table 1. Electrical losses

Water sample	Resistivity, Ω-cm	Power loss, kw	Power loss, %
Pure	20,000	0.036	0.0024
City water (Pasadena, California)	4,000	0.179	0.012
550 ppm Sodium nitrite	238	3.02	0.20
1400 ppm Sodium nitrite	200	3.46	0.24

The magnet is designed so a pump must maintain a pressure of about 130 psi in order to circulate the required amount of water. The distilled water circuit contains pressure switches which cut the excitation for the armature circuit of the dc generator when the water pressure falls below 100 psi.

Pasadena, California city water was not used to cool the magnet because it contains calcium and magnesium salts. Consequently, an existing closed-loop system of distilled water was used. The complete system contains the magnet, a cooling tower, pumps, and a heat exchanger. The cost of water pumps was diminished by locating the laboratory in the vicinity of existing wind tunnel facilities. A mercury manometer from an orifice plate flow meter is mounted near the instrument control panel.

Since the noise level of the generator is excessive, it was fully enclosed in a separate room. An appreciable magnetic field due to the magnet and bus bars penetrates nearby rooms to a depth of about 30 ft. This stray field amounts to several hundred gauss just outside the magnet; any iron which might be attracted to the magnet must be removed from the area. Attraction forces are very large inside the air core of the magnet. It is generally assumed that exterior magnetic fields have no biological effect on the occupants of the laboratory.

V. THE MAGNET SOLENOID

The magnet is intended to give high magnetic field strengths for continuous operation over indefinite periods. The magnet is mounted with its axis vertical. The central tube for the magnet is 2 in. ID.

Since the magnet has to dissipate 2 Mw, the coil is about 17 in. OD and provision is made for internal cooling. This is done by forcing water radially through 0.025-in. high spaces between successive turns of the coil (shown in Fig. 6). These passages are maintained by spacers in such numbers as to allow removal of heat generated in their immediate vicinity at the rate of about 200 w/cm^2 of cooling surface. Thus, the temperature at the inner portion of the magnet can be held below the boiling point of water. The flow of water is turbulent. The Reynolds number is a million (well above its critical value). The resistance of the magnet is about 220 $\mu\Omega$ and the field constant is just over 1 gauss/amp.

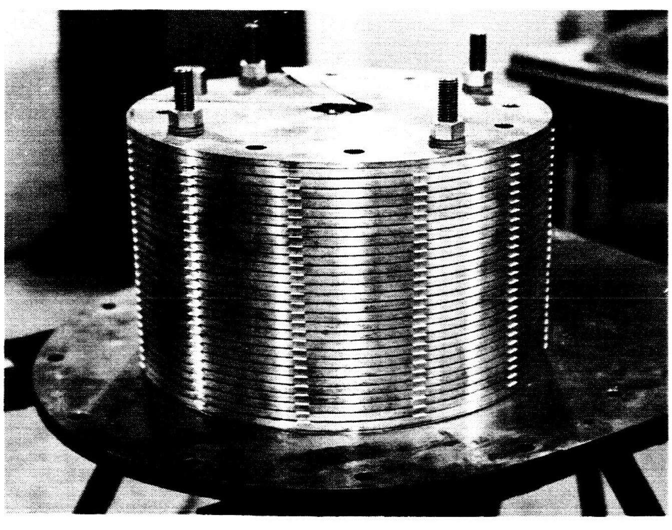

Fig. 6. Solenoid and bottom bus

Each of the copper turns of the magnet is 0.318-in. thick and together form a continuous solenoid of 27.2 turns. The solenoid and electrical insulation spacers are held together simply by mechanical pressure. Only the end turns of the solenoid are backfilled with copper sheet and attached to heavier copper plates (Fig. 7) which are bolted to the bus. Micarta gaskets prevent the coil from touching the inner tube or the outer case, and allow water to circulate over the surfaces of the coil. Holes of ¾-in. D penetrate the coil near its outer edge. Micarta tubes in these holes prevent the bolts and coil from moving or touching each other. These tubes have holes machined in the wall to allow water to circulate and to prevent local burning. The present design for an average heating rate of only 200 w/cm^2 is quite safe from forming a steam layer at the cooling interfaces. The surface heating rate at the inner radius position of the solenoid is calculated to be about 1,200 w/cm^2. This is about one/fourth of the heating rate for forming steam layers.

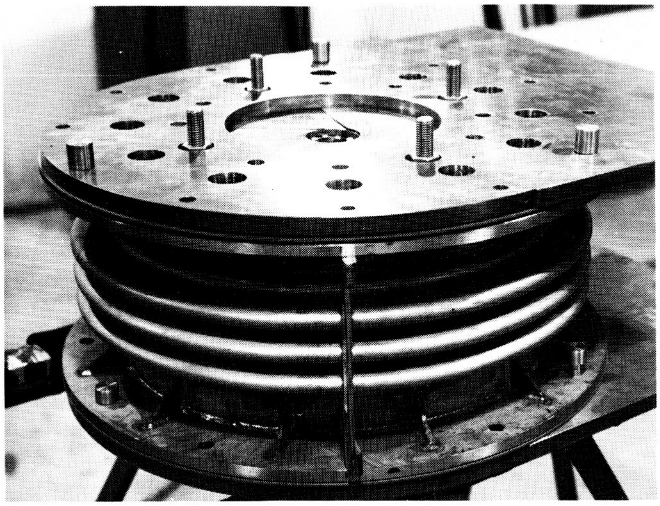

Fig. 7. Magnet expansion section

Other magnets could be designed with much smaller cooling surfaces if higher operating temperatures were used. An upper limit heating rate of about 5,000 w/cm^2 might be obtainable before steam layer formation would cause the magnet to blow up.

The design parameters for the solenoid are as follows:

Current, $I = 95{,}000$ amp

Power, $w = 2.0 \times 10^6$ w

Inside radius, $r_1 = 1.25$ in.

Outside radius, $r_2 = 8.5$ in.

Turn thickness, $t + t_1 = 0.343$ in.

Voltage, $V = 21$ v

Resistivity $= 2.15 \times 10^{-6}$ ohm-cm

@ 60°C $= 8.50 \times 10^{-7}$ ohm-in

Coil length, $L = 10$ in.

Plate thickness $t = 0.318$ in.

Water channel $t_1 = 0.025$ in.

$$\text{Parameter } \alpha = r_2/r_1 = 8.5/1.25 = 6.8 \qquad (4)$$

$$\text{Parameter } \beta = L/2r_1 = 10/2(1.25) = 4.0 \qquad (5)$$

$$\text{Turns } N = \left[L - 2\,(t + t_1)\right]/(t + t_1) = 27.2 \qquad (6)$$

$$\text{Space factor } \lambda = t/(t + t_1) = 0.318/0.343 = 0.925 \qquad (7)$$

The current density at the inner radius position with r_1 is given in centimeters.

$$J_1 = (4\pi\beta \ln \alpha)^{-1/2} (W/\rho\lambda r_1^{3})^{1/2} = 18{,}000 \text{ amp/cm}^2 \qquad (8)$$

The total effective magnet resistance is

$$R_1 = 2\pi\rho \left[L - 2(t + t_1)\right]/t(t + t_1) \ln (r_2/r_1) = 219\mu\Omega \qquad (9)$$

The first axial field strength equation with r_1 given in centimeters is (Ref. 2)

$$H = G\,(W\lambda/\rho r_1)^{1/2} = 101{,}000 \text{ gauss} \qquad (10)$$

The dimensionless Fabry factor, used with Eq. (10), is

$$G = \left[\sqrt{\pi}/5\right] \cdot (\beta \ln \alpha)^{-1/2} \ln \left[(\alpha)\,(\beta + \sqrt{1 + \beta^2})/(\beta + \sqrt{\alpha^2 + \beta^2})\right] = 0.196 \qquad (11)$$

The second axial field strength equation, with coil height L given in centimeters is

$$H = 4\pi NIS/10\,L = 102{,}000 \text{ gauss} \qquad (12)$$

The dimensionless shape factor, used with Eq. (12), is

$$S = 1 - (\log r_2/r_1)^{-1} \log\left[(1 + \sqrt{1 + (2r_2/L)^2})/(1 + \sqrt{1 + (2\,r_1/L)^2})\right] = 0.802 \qquad (13)$$

The solenoid axial compression force at the inner radius, r_1, is

$$F_1 = 2 \times 10^{-9}\left[\frac{\pi N r_1 I}{L}\right]^2 \frac{\text{j}}{\text{cm}}\left[\frac{10^7 \text{ dyne cm}}{\text{j}}\right]\left[\frac{2.25 \times 10^{-6} \text{ lb}}{\text{dyne}}\right]$$

$$= 2 \times 10^{-9}\left[\frac{\pi(27.2)\,(1.25)\,(95{,}000 \text{ amp})}{(10)}\right]^2 (10^7)\,(2.25 \times 10^{-6}) = 46{,}300 \text{ lb} \qquad (14)$$

This 23-ton axial compression must be supported by the dielectric spacers placed radially throughout the coil, 30 deg apart. These spacers are made of silicone-fiberglas. They are 3/16-in. wide at the inner radius, ½-in. wide at the outer radius, and 0.025-in. thick. No deformation of the spacers was observed.

A more conservative calculation can be shown from the energy stored in the magnetic field. This is also the energy expended in producing such a field. The energy (in joules) stored in the magnetic field can be expressed as

$$W = 5 \times 10^{-9} \pi HNI r_1^2 \tag{15}$$

Dividing this expression by $(L - 2(t + t_1) + Sr_1)$, gives the axial compressive force at the inner radius position F_1, where L = coil length, S = dimensionless factor given by Eq. (13), and r_1 = inner radius.

$$F_1 = W/(L - 2(t + t_1) + Sr_1) \text{ joules}$$

$$= \frac{(5 \times 10^9)\pi(10^5)(27.2)(95{,}000)(3.18)^2 \text{ j}}{[25.4 \text{ cm} - 0.736 \text{ cm} + (0.802)(3.18 \text{ cm})]}$$

$$= \left[\frac{1640 \text{ j}}{\text{cm}}\right]\left[\frac{10^7 \text{ dyne cm}}{\text{j}}\right]\left[\frac{2.25 \times 10^{-6} \text{ lb}}{\text{dyne}}\right]$$

$$= 36{,}900 \text{ lb} \tag{16}$$

The dielectric spacers must support the above compressive load without deforming the surface of the copper turns. No permanent deformation of the copper was observed after operating the magnet.

A second internal stress of great importance to the design is the radial expansion stress due to the ponderomotive forces within the coil. An analytical expression for this force is given by (Ref. 3)

$$F_2 = H^2/8\pi \text{ g dyne/cm}^2$$

$$= \frac{(10^5 \text{ gauss})^2}{8\pi(980 \text{ cm/sec}^2)} \cdot (\text{gm/cm sec}^2)(\text{lb}/450 \text{ g})(6.45 \text{ cm}^2/\text{in}^2)$$

$$= 5{,}770 \text{ lb/in}^2 \tag{17}$$

This stress can be treated as an internal pressure in a thick-walled pipe. The mass of the solenoid and bolting arrangement control this pressure in addition to the 130 lb/in.^{2} internal water pressure. The total amount of internal pressure the system must support is 5,900 lb/in.^{2} when the magnet is operating at 100 kilogauss.

As a check on this calculation, the dot product of the field strength and current density can be integrated over the volume of the coil. This computation produces the outward ponderomotive thrust at the inner radius when Eq. (8) is used for the current density.

$$F_2 = \int_r (H\, j)\, dv$$

$$= 8\pi^2 \lambda t\, j_1^2 \int_{r_1}^{r_2} r^2 \ln(r_2/r)\, dr$$

$$= 8\pi^2 \lambda t\, j_1^2 \left[\frac{(r_2^3 - r_1^3)}{9} - \frac{r_1^3}{3} \ln(r_2/r_1)\right]$$

$$= 8\pi^2 (0.925)(0.8 \text{ cm}) \left[\frac{1800\, AB \text{ amp}}{\text{cm}^2}\right]^2 (1120 \text{ cm}^3 - 20 \text{ cm}^3)$$

$$= 2.08 \times 10^{11} \text{ dyne } (2.2 \text{ lb}/10^6 \text{ dyne}) = 457{,}000 \text{ lb} \tag{18}$$

This force is divided by the surface area of the inner portion of the coil to obtain the force per unit area. Since, the surface $= \pi Dh = \pi(2.50 \text{ in.})(10 \text{ in.}) = 78.5 \text{ in.}^2$,

$$F_2 = \frac{457{,}000 \text{ lb}}{78.5 \text{ in.}^2} = 5{,}830 \text{ lb/in}^2 \tag{19}$$

This computation checks Eq. (17) within 1%.

VI. CRYOGENIC MAGNET DEWAR

A commercial cryogenic dewar was modified for use with the electromagnet. This dewar has a nitrogen cooled shield enclosing a helium container. The exterior of the lower section of the dewar forms the wall of the air core magnet as shown by Fig. 8. The entire dewar is removable by unseating an O-ring gasket water seal on the lower section of the dewar and removing the cover plate bolts at the top of the magnet.

The cryogenically cooled test section is 14-in. long and has an ID of 1.5 in. reaching to the center of the magnet. The helium container has a radiation shield cooled by 4.7 l of liquid nitrogen. A vacuum pump is mounted on the roof of the laboratory and will be used to pump on the helium volume so that experiments can be carried out below 4°K. This vacuum pump will be operated continuously during such tests. The helium-filled lower section is supplied with 2.25 l of liquid which is stored in the upper portion of the container. The dewar forms an integral part of the magnet and can be used to simultaneously test materials under intense magnetic fields and cryogenic temperatures.

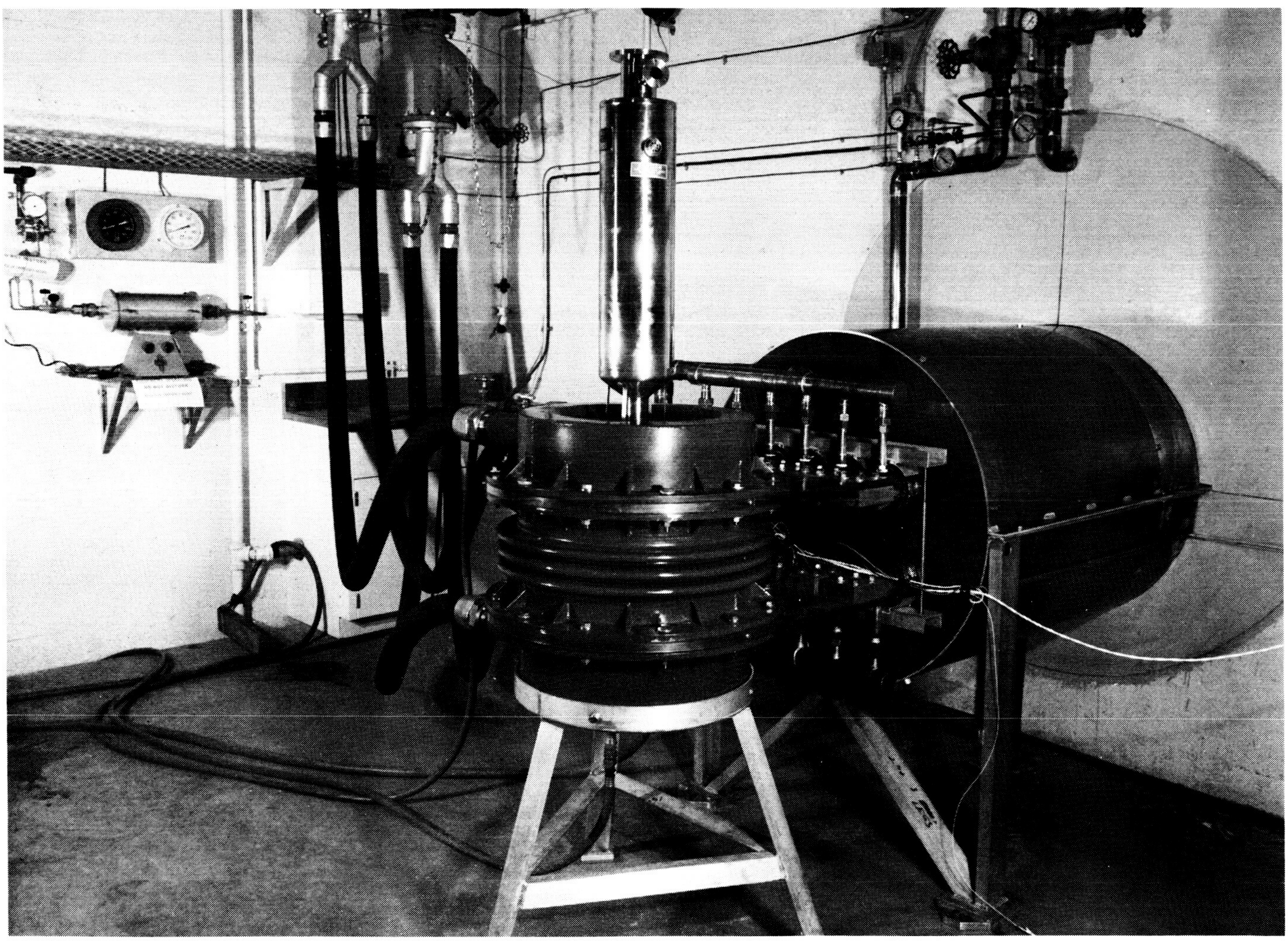

Fig. 8. Complete magnet-Dewar assembly

VII. STABILITY AND PERFORMANCE

Many of the experiments contemplated for the high-field magnet require magnetic field stabilities of one part in 10^4 to 10^5 over periods of several minutes. Therefore, a rather extensive program has been initiated to measure the magnetic field stability and determine if the stability is adequate and if any improvements can be made in the magnet's performance.

Initial measurements of the magnetic field were made with a Rawson rotating coil gaussmeter. These measurements indicated that the magnetic field measured in the coil center vs the current through the magnet and voltage across the magnet followed very close to the values anticipated in the range from 0 to 97 kilogauss. In addition, no gross instabilities (2 parts in 10^2) in the field were observed in the 0- to 97-kilogauss range with the Rawson gaussmeter. However, the Rawson meter has an absolute accuracy of only 2% and a differential accuracy of about 1%.

Attempts were made to measure the magnetic field at low levels (approximately 10,000 gauss) with a nuclear magnetic resonance (NMR) gaussmeter. The absolute values of the field could be measured to one part in 10^5; however, no resonance signal was detected from the NMR gaussmeter. The failure to detect the NMR signal could result from a large magnetic field inhomogeneity, one part in 10^3 over one centimeter, or a magnetic field instability of one part in 10^3.

A Bell differential gaussmeter (a Hall probe) capable of measuring relative changes in the field of two parts in 10^4 at 10,000 gauss was placed in the magnet. Figure 9 shows the results of this measurement. It can be seen that the field changed 50 gauss (5 parts in 10^3) in a period of several seconds. These fluctuations in the magnetic field were larger than expected and attempts have been made to ascertain their origin and to correct the difficulty.

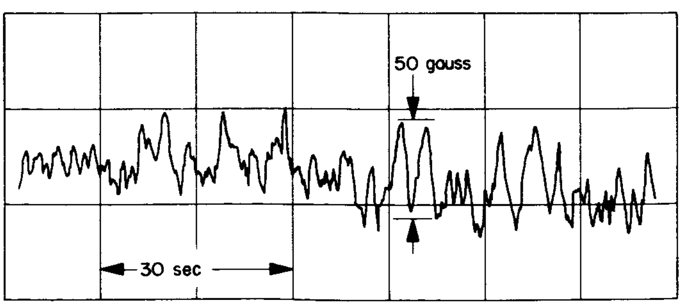

Fig. 9. Magnetic field fluctuations

It was known that the cooling water had a larger conductance than has normally been used for this type of magnet. In addition, fluctuations were observed in the water pressure to the magnet which were approximately of the same frequency as the fluctuation in the magnetic field. It was therefore assumed that the cooling water might be a possible source of instability in the magnetic field. The magnet was operated with Pasadena city water at a low flow rate of approximately 10 gal/min and a more constant pressure. Unfortunately, under these operating conditions, the magnetic field still showed the fluctuations as described before. It was determined that the cooling water was not the cause of the field instability. It was thought that the generator itself must have been the cause of the fluctuation in the field. The generator voltage was back-biased by a battery, and a 50-mv full scale strip chart recorder was connected across the generator. The results of these measurements are shown in Fig. 10. It was observed that 10-mv fluctuations at an output of 1.25 v from the generator were present. A correlation between the changes in the generator voltage and the magnetic field was also noted.

A well-regulated (1 part in 10^5) power supply was then used to excite the excitation coils of the unipolar generator; however, again fluctuations of the magnetic field

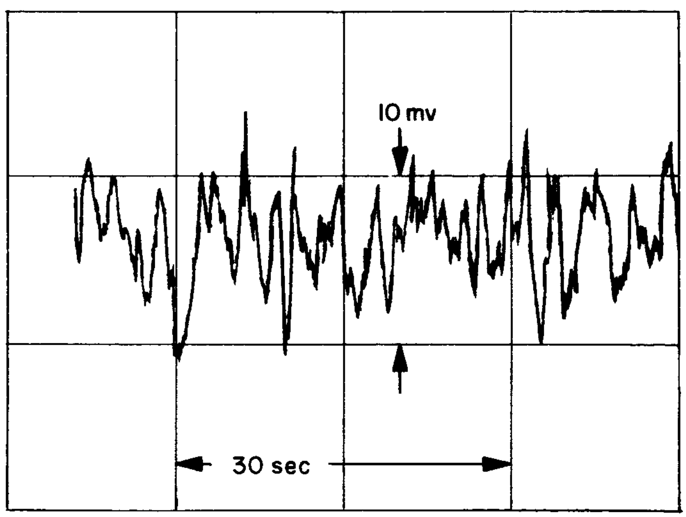

Fig. 10. Generator-voltage fluctuations

of the magnet and the output voltage of the generator were observed. In addition, the rotational speed of the generator was monitored with a stroboscope and no change was noted.

The generator was also operated without a load and the output voltage fluctuated approximately 1 mv with a period of 2 sec at an output voltage of 7.95 v. It is therefore thought that the fluctuations in the output voltage of the generator result from changes in the impedance of the NaK brushes in the generator. Further measurements have shown that most of the changes in output voltage of the generator originate from the inboard current collector nearest to the motor.

The Bell gaussmeter has a response time of about 0.5 sec. Therefore, high frequency fluctuations could not be observed with this instrument. Figure 11 shows the results of measurements from a pickup coil of 600 turns with a mean radius of 1 cm placed at the center of the magnet. This coil was connected directly to an oscilloscope. A ⅛-in. thick copper and aluminum cylindrical

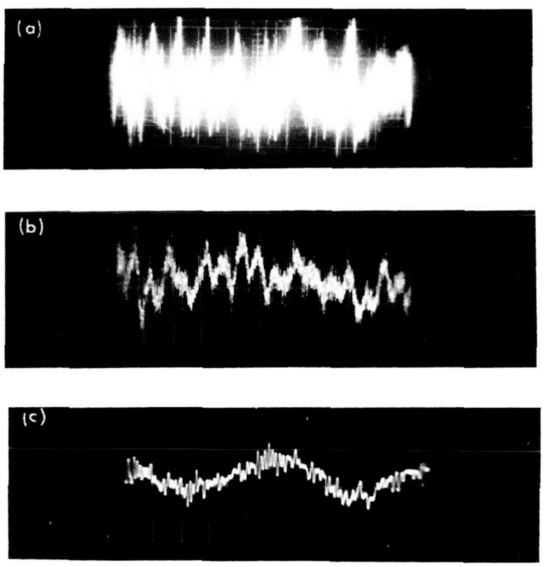

Fig. 11. Unshielded pickup coil: (a) 10 msec/cm, 20 mv/cm; (b) 1 msec/cm, 20 mv/cm; (c) 0.1 msec/cm, 20 mv/cm

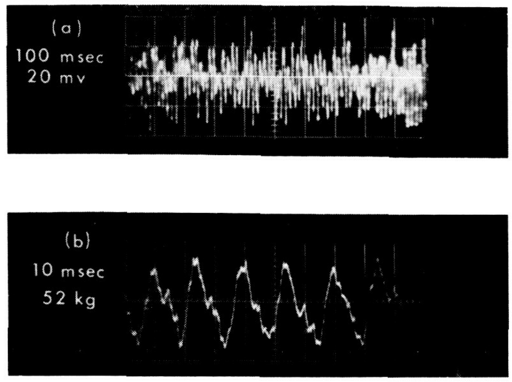

Fig. 12. Shielded pickup coil: (a) 100 msec/cm, 20 mv/cm; (b) 10 msec/cm, 20 mv/cm

tube was placed concentric in the port of the magnet with the pickup coil inside the two cylinders. These tubes attenuated the higher frequency components of the field fluctuations and facilitated the measurement of low frequency changes in the magnetic field (shown in Fig. 12). From a knowledge of the geometry of the pickup coil and the voltage induced in the coil, it was possible to calculate the changes in the magnetic field of the magnet. The results are summarized in Table 2, along with the data from the Bell gaussmeter.

The power consumption of the magnet is very close to that predicted by design calculations for any particular magnetic field strength. For a magnetic field of 92 kilogauss, and for the parameters $G = 0.196$, $\lambda = 0.925$, $r_1 = (1.25 \text{ in.})(2.54 \text{ cm/in.}) = 3.18$ cm, and $\rho = 2.15 \times 10^{-6}$ Ω-cm at 60°C (140°F) for 90% IACS copper, a power of 1.63 Mw is required. This compares with the experimental power of 1.65 Mw (19.4 v and 85 kiloamps) at 92 kilogauss.

Table 2. Magnetic field fluctuations

Fluctuation, ΔB gauss	Intensity, B gauss	Variation, $\frac{\Delta B}{B}$	Period (time for ΔB), sec	Method of measurement of ΔB field
50	10,000	5×10^{-3}	1–3	Bell gaussmeter
25	52,000	5×10^{-4}	10^{-2}	pickup coil
5	52,000	1×10^{-4}	10^{-3}	pickup coil
0.01	52,000	2×10^{-7}	10^{-5}	pickup coil

VIII. MAGNET FACILITY USE PROGRAM

This facility will be used first for low temperature research. Specifically, the current density vs magnetic field will be measured for superconductors in the vicinity of 80 kilogauss. The availability of such high fields in a fairly large test volume suggests a number of experiments in the demagnetization region for calorimetry, superconductivity, etc. Such a high field also offers an opportunity for measurements of time resolved spectroscopy.

The facility could be used for cyclotron resonance investigations of new materials. Fundamental information about basic electronic properties can be obtained which would not be possible at lower magnetic field strengths. Experiments with intermetallic compounds of the Types III-V, and II-VI hold promise in high magnetic fields.

Improved resolution can be obtained in optical Zeeman effect measurements at 100-kilogauss fields. Even higher fields would be very useful. Zeeman effect measurements have assumed great importance for observing excitons in semiconductors.

Magneto-optic measurements in the far infrared will be possible for relatively impure materials, at 100-kilogauss fields, where sufficient line separation can be achieved in spite of impurity line broadening.

Measurements for the De Haas Van Alphen effect on semimetals can be made in 100-kilogauss fields. Magnetoplasma effects in solids could be studied. Much of the same information for solids would be of value for studies of dense plasmas in gas discharges.

REFERENCES

1. McAdams, W. H., *Heat Transmission,* 3rd edition, New York, 1954.
2. Montgomery, D. B., and Terrell, J., "Some Useful Information for the Design of Air-Core Solenoids," *MIT National Magnet Laboratory, AFOSR-1525,* 3rd printing, 1962.
3. Kolm, H. H., et al., "High Magnetic Fields," *Proceedings of the MIT International Conference on High Magnetic Fields,* John Wiley and Sons, New York, p. 93, 1962.

ACKNOWLEDGMENT

The authors would like to acknowledge the help and continued interest of Dr. A. F. Hildebrandt, who initiated the work on this intense magnetic field laboratory. The authors would also like to express their gratitude to Dr. R. J. Mackin for his interest and support in the design of the magnet. Very helpful consultations were held with Dr. H. H. Kolm at the MIT National Magnet Laboratory during the beginning of this program. The authors also wish to thank Mr. John C. Fakan of NASA Lewis Research Center for his assistance in bringing this facility on line during the startup period.